

Studies on Dysbiosis of Gut Microbiota in *Drosophila*

関原, 早苗

<https://doi.org/10.15017/1806833>

出版情報 : 九州大学, 2016, 博士 (理学), 課程博士
バージョン :
権利関係 : 全文ファイル公表済

Studies on Dysbiosis of Gut Microbiota in *Drosophila*

Sanae Sekihara

Graduate School of Systems Life Sciences,

Kyushu University, Fukuoka, Japan

2016

(平成 28 年度)

CONTENTS

	Page
ABBREVIATIONS	3
ABSTRACT.....	4
INTRODUCTION.....	5
RESULTS	7
DISCUSSION.....	14
EXPERIMENTAL PROCEDURES	17
REFERENCES	25
FIGURE LEGENDS	32
TABLES.....	36
FIGURES.....	42
ACKNOWLEDGEMENTS.....	51

ABBREVIATIONS

TG	transglutaminase
IMD	immune deficiency pathway
AMPs	antimicrobial peptides
ROS	reactive oxygen species
DUOX	dual oxidase
IMD-AMPs	immune deficiency pathway-controlled antimicrobial peptides.

ABSTRACT

We recently reported that transglutaminase (TG) suppresses immune deficiency pathway-controlled antimicrobial peptides (IMD-AMPs), thereby conferring immune tolerance to gut microbes, and that RNAi of the *TG* gene in flies decreases the lifespan compared with non-*TG*-RNAi flies. Here, analysis of the bacterial composition of the *Drosophila* gut by next-generation sequencing revealed that gut microbiota comprising one dominant genus of *Acetobacter* in non-*TG*-RNAi flies was shifted to that comprising two dominant genera of *Acetobacter* and *Providencia* in *TG*-RNAi flies. Four bacterial strains, including *Acetobacter persici* SK1 and *Acetobacter indonesiensis* SK2, *Lactobacillus pentosus* SK3, and *Providencia rettgeri* SK4, were isolated from the midgut of *TG*-RNAi flies. SK1 exhibited the highest resistance to the IMD-AMPs Cecropin A1 and Dipterecin among the isolated bacteria. In contrast, SK4 exhibited considerably lower resistance against Cecropin A1, whereas SK4 exhibited high resistance to hypochlorous acid. The resistance of strains SK1-4 against IMD-AMPs in *in vitro* assays could not explain the shift of the microbiota in the gut of *TG*-RNAi flies. The lifespan was reduced in gnotobiotic flies that ingested both SK4 and SK1, concomitant with the production of reactive oxygen species and apoptosis in the midgut, whereas survival rate was not altered in gnotobiotic flies that mono-ingested either SK4 or SK1. Interestingly, significant amounts of reactive oxygen species were detected in the midgut of gnotobiotic flies that ingested SK4 and SK2, concomitant with no significant apoptosis in the midgut. In gnotobiotic flies that co-ingested SK4 and SK1, an additional unknown factor(s) may be required to cause midgut apoptosis.

INTRODUCTION

Foreign substances, including foods, minerals, and microbes, continually pass through the intestinal tract and attach to the gut epithelium. Development of physical and immunologic barriers against foreign substances is thus essential to protect the gut epithelia. Healthy and balanced gut microbiota provide essential nutrients for their host and help to maintain gut immune homeostasis, whereas disruption of the balance, called dysbiosis, is associated with various animal diseases (1, 2). The fruit fly, *Drosophila melanogaster*, is a useful model for investigating the close relationship between bacteria and host and bacteria interactions (3, 4), and the gut microbial community of *Drosophila* comprises $\sim 10^5$ microbes of ~ 20 species (5–7). The *Drosophila* gut is functionally analogous to the mammalian intestinal tract (8, 9), producing antimicrobial peptides (AMPs) and reactive oxygen species (ROS) (10, 11). Microbes or microbe-derived immune elicitors in the fly gut can initiate several immune signaling pathways, such as the immune deficiency (IMD)-pathway activated by peptidoglycans to produce AMPs and the dual oxidase (DUOX) signaling pathway activated by uracils to produce ROS (11–14). In addition to pathogenic bacteria, commensal microbe-derived peptidoglycans constitutively activate the IMD pathway in the gut through peptidoglycan recognition protein-LC and peptidoglycan recognition protein-LE, and several types of suppression of the IMD pathway have been reported (10, 15). On the other hand, non-commensal bacteria, such as the opportunistic insect pathogen *Ecc15*, and the insect pathogens *Pseudomonas entomophila* and *Gluconobacter morbifer* G707T, secrete uracil to trigger the DUOX-dependent ROS production (16). The IMD pathway-controlled antimicrobial peptides

(IMD-AMPs) exhibit a microbicidal effect on a narrow range of virulent bacteria, whereas ROS-based immunity appears to be a more effective anti-microbial system against gut infection (11–14).

Transglutaminase (TG) catalyzes the isopeptide bond formation between Lys and Gln residues in a Ca^{2+} -dependent manner (17). In mammals, eight TG isozymes are involved in various biologic processes, such as blood coagulation, extracellular matrix formation, and apoptosis (18). In invertebrates, such as horseshoe crabs, crayfish, and *Drosophila*, TG-mediated crosslinking of specific proteins is involved in hemolymph coagulation and cuticle formation (19–22). *Drosophila* carries a single *TG* gene, which crosslinks the nuclear factor- κ B-like transcription factor Relish in the IMD pathway in midgut cells to suppress the expression of antimicrobial peptides (23). RNAi of the *TG* gene enhances the expression of IMD-AMPs, including Cecropin A1 and Diptericin, which decreases the lifespan concomitant with apoptosis of the midgut cells, compared with non-*TG*-RNAi flies (23). Interestingly, *TG*-RNAi does not decrease the lifespan of germ-free flies, whereas non-*TG*-RNAi flies that ingest gut lysates prepared from conventionally reared *TG*-RNAi flies have a short lifespan (23). We hypothesized that *TG*-RNAi causes dysbiosis of the gut microbiota, leading to a short lifespan. Here we identified the bacterial composition in the gut of *TG*-RNAi and non-*TG*-RNAi flies by next-generation sequencing, and characterized the microbes isolated from the gut.

RESULTS

Effects of TG-RNAi on gut flora – The survival rates of conventionally reared *TG*-RNAi (*Da>TG IR*) and non-*TG*-RNAi (*Da>+*) flies as control flies are shown in Figure 1, which confirmed that RNAi directed against the *TG* gene reduces the lifespan of flies under conventional non-sterile conditions (23). To investigate the effects of *TG*-RNAi on the gut microbiota, gut microbes of 0.5-day-old and 10-day-old non-*TG*-RNAi or *TG*-RNAi flies were analyzed using next-generation sequencing of 16S rRNA gene (rDNA) clones. Four genera of bacteria were identified in both non-*TG*-RNAi and *TG*-RNAi flies, including *Acetobacter*, *Lactobacillus*, *Providencia*, and *Wolbachia* (Table 1). These genera were previously reported as bacterial communities in *D. melanogaster* (24–30). Bacteria that highly matched the sequences of the V4 region of the 16S rDNA clones are shown in Table 2. In this study, *Wolbachia* is not discussed because it is an endosymbiont bacteria, not a gut microbe (31). The effective number of bacterial cells was estimated as described in “EXPERIMENTAL PROCEDURES”. In 0.5-day-old non-*TG*-RNAi flies, the most dominant genus was *Acetobacter*, followed by *Providencia* (Fig. 2A, left panel). In 0.5-day-old *TG*-RNAi flies, *Providencia* was the most dominant, followed by *Acetobacter* (Fig. 2A, right panel). *Lactobacillus* was a recessive genus in both cases in 0.5-day old flies (Fig. 2A, right and left panels). *Acetobacter* became more dominant, whereas *Providencia* and *Lactobacillus* were not identified in 10-day-old non-*TG*-RNAi flies in the sequencing analysis (Fig. 2B, left panel). Interestingly, microbiota in 10-day-old *TG*-RNAi flies contained two bacterial dominant microbiota, *Acetobacter* and *Providencia*, at a ~1:1 ratio in the gut (Fig 2B, right panel). To determine whether the total number of gut

bacteria was changed by *TG*-RNAi, the copy number of the 16S rDNA was analyzed by quantitative PCR (qPCR) after considering the 16S rRNA copy number of each genus (Fig. 2C). The total number of gut bacteria did not differ significantly between 0.5-day-old non-*TG*-RNAi and 0.5-day-old *TG*-RNAi flies, whereas the bacterial load was increased 10-fold in 10-day-old *TG*-RNAi flies compared to 10-day-old non-*TG*-RNAi flies, suggesting that dysbiosis of the gut microbiota was induced by *TG*-RNAi to increase the number of gut microbes compared to that in non-*TG*-RNAi flies. We previously reported that *TG*-RNAi enhances the expression of IMD-AMP genes such as *Cecropin A1* and *Diptericin* (23). To confirm the induction of IMD-AMPs by *TG*-RNAi, the expression of *Cecropin A1* was measured by qPCR. No difference in the expression of *Cecropin A1* was observed in the guts of 0.5-day-old flies between non-*TG*-RNAi and *TG*-RNAi flies, whereas in 10-day-old flies, the expression of *Cecropin A1* was significantly increased in *TG*-RNAi flies, but not in non-*TG*-RNAi flies (Fig. 2D).

Antimicrobial peptide-resistance of the isolated bacteria – IMD-AMPs in the *Drosophila* gut act as a selective pressure and overexpression of IMD-AMPs induces dysbiosis, although the importance of IMD-AMPs in immune responses in the gut is unclear (12, 24). We speculate that *TG*-RNAi triggers a shift in the gut microbiota from the single bacterial dominant microbiota of *Acetobacter* to the two bacterial dominant microbiota of *Acetobacter* and *Providencia* through regulation of the production of IMD-AMPs. We isolated gut bacteria from 10- to 12-day-old non-*TG*-RNAi or *TG*-RNAi flies by plating and incubating gut homogenates on Hestrin-Schramm medium agar plates and nutrient agar medium plates. Four bacterial strains were isolated from the midgut of the flies; the SK1 and SK3 strains were

isolated from both non-*TG*-RNAi and *TG*-RNAi flies, and the SK2 and SK4 strains were isolated from *TG*-RNAi flies, but not from non-*TG*-RNAi flies. Sequence analyses of the entire 16S rDNAs identified these isolated strains (SK1, SK2, SK3, and SK4) as *Acetobacter persici*, *Acetobacter indonesiensis*, *Lactobacillus pentosus*, and *Providencia rettgeri*, respectively (Table 3).

To evaluate the colonization ability of strains SK1-4, bacterial loads in the midguts of germ-free *TG*-RNAi or germ-free non-*TG*-RNAi flies that transiently ingested each bacterial strain were examined (Fig. 3). SK1 and SK4 colonized equally in the midguts of both non-*TG*-RNAi and *TG*-RNAi flies. In contrast, little or no bacterial load of SK2 and SK3 was found in non-*TG*-RNAi flies, especially the middle and posterior midgut regions, but sufficient bacterial loads of SK2 and SK3 were counted in the midguts of *TG*-RNAi flies. These findings suggest that a better intestinal habitat is provided for specific bacterial strains under the conditions of *TG*-RNAi despite the increasing expression of IMD-AMPs in the fly gut. To investigate the resistance of strains SK1-4 to IMD-AMPs, the antimicrobial activities of Cecropin A1 and Diptericin were assayed (Figs. 4 and 5 and Table 4). SK1 exhibited the strongest resistance to Cecropin A1 with an IC_{50} value of $>10 \mu\text{g/mL}$ in isolated and established bacteria (Fig. 4 and Table 4). The IC_{50} value of SK2 and SK3 to Cecropin A1 was an order of magnitude higher ($0.22\sim 0.35 \mu\text{g/mL}$) than the IC_{50} values of established bacteria ($0.05\sim 0.06 \mu\text{g/mL}$; Fig. 4 and Table 4). In contrast, SK4 exhibited considerably lower resistance against Cecropin A1 with an IC_{50} of $0.07 \mu\text{g/mL}$, similar to that of established bacteria (Fig. 4 and Table 4). Notably, Diptericin had no or little inhibitory effect on the growth of SK1 or SK3 at a concentration of $20 \mu\text{g/mL}$ (Fig. 5 and Table 4). SK4 also had

significantly higher resistance to Diptericin than the established bacteria, including *Erwinia carotovora carotovora* 15 2141, *Pseudomonas azotoformans* IAM 1603, and *Escherichia coli* K12 (Fig. 5 and Table 4). *Providencia alcalifaciens* JCM1673T, belonging to the same genus of SK4, exhibited rather high resistance to Diptericin (Fig. 5 and Table 4).

No experimental conditions to culture all microbial communities in the fly gut have been established and strains SK1-4 may not reflect the complete microbiome of *TG*-RNAi flies. *Gluconobacter morbifer* G707T is reported to be a microbe with pathologic consequences in the *Drosophila* gut (24). *G. morbifer* G707T and reported intestinal strains, including *Commensalibacter intestini* A911T, *Acetobacter pomorum*, *Lactobacillus brevis* EW, and *Lactobacillus plantarum* WJL (24), could be cultured under the same conditions used for SK1, and their antimicrobial resistance was examined (Table 5). *G. morbifer* G707T exhibited significantly lower resistance against Cecropin A1 at 1.0 µg/mL, compared with the other commensal stains, whereas Diptericin at 10 µg/mL had little effect on the growth of *G. morbifer* G707T. On the other hand, in this study, the genera *Gluconobacter* and *Commensalibacter* were not identified in the midguts of non-*TG*-RNAi and *TG*-RNAi flies by next-generation sequencing of 16S rDNA. Therefore, we used strains SK1-4 as representative microbiota of *TG*-RNAi flies.

Anti-ROS activities of the isolated bacteria – In *Drosophila*, midgut cells may be tolerant toward commensal bacteria and at the same time they should be protected against the invasion of virulent pathogens. The *Drosophila* genome contains one *DUOX* gene, which is indispensable for gut immunity, and an extracellular peroxidase homology domain of *DUOX* has the enzymatic activity to produce highly

microbicidal hypochlorous acid (HOCl) from H₂O₂ in the presence of chlorine (32). On the other hand, severe gut infection by pathogenic bacteria induces excessive production of DUOX-dependent ROS to damage host tissues and cells, and thus decreases the survival rate (11, 16). Strains SK1-4 were incubated in the presence of HOCl containing 15 µg/L or 50 µg/L available chlorine to determine the resistance to ROS (Table 6). Treatment with 15 µg/L of HOCl had little or no effect on strains SK1-4. Furthermore, SK1 and SK4 were quite resistant to HOCl at a higher concentration of 50 µg/L. On the other hand, the growth of SK3 was strongly suppressed at 50 µg/L of HOCl. These findings suggest that SK1 and SK4 acquire high resistance against ROS in the *Drosophila* gut. Moreover, the intestinal strains of *A. pomorum* and *L. brevis* EW, and the insect opportunistic pathogen *Ecc15* 2141 exhibited very high anti-ROS activity at 50 µg/L of HOCl (Table 6). In contrast, *C. intestini* A911T, *E. coli* K12, and *P. alcalifaciens* JCM1673T were highly sensitive to HOCl under the same conditions (Table 6).

Effects of long-term ingestion of strains SK1-4 on survival rates and midgut apoptosis – Gut bacteria are important for maintaining host homeostasis by generating nutrients and inhibiting the growth of invading pathogens (2, 33, 34). In *Drosophila*, a strain of *A. pomorum* plays an important role in host homeostatic programs such as body size and energy metabolism by activating insulin/insulin-like growth factor signaling (35). To examine the effects of the ingestion of strains SK1-4 on the fly survival rate, gnotobiotic flies were prepared by long-term feeding in germ-free flies. Survival rate experiments using gnotobiotic flies revealed that mono-ingestion of strains SK1-4 for 25 days had little effect on the survival rates (Fig. 6A). Interestingly, in gnotobiotic flies, co-ingestion of SK4 and SK1 significantly decreased

the survival rate, whereas co-ingestion of SK4 and SK2 had little effect. To examine the colonization ability of strains SK1-4 in the long-term ingestion experiments, bacterial loads of gnotobiotic flies that mono-ingested or co-ingested strains SK1-4 were counted at 15 and 25 days after ingestion (Fig. 6B). After 25 days ingestion, each strain exhibited sufficient colonization with $10^4 \sim 10^5$ colony forming units (CFUs)/gut whether mono- or co-ingested. Bacterial loads of mono-ingested strains SK1-3 after 25 days ingestion were 10-times greater than those after 15 days ingestion. The phenomenon of an age-dependent bacterial load increase in the midgut was reported previously (29).

We previously performed TUNEL assays and detected apoptotic cells in the middle midgut of conventionally reared *TG*-RNAi flies, but not in conventionally reared non-*TG*-RNAi flies or germ-free *TG*-RNAi flies (23). To evaluate the effects of long-term ingestion of strains SK1-4 on apoptosis of midgut cells, we performed TUNEL assays after 18 days ingestion. The number of TUNEL-positive guts was significantly increased in the middle midgut region of gnotobiotic flies that co-ingested SK4 and SK1 compared with gnotobiotic flies that mono-ingested SK4 or co-ingested SK4 and SK2 (Fig. 7). Therefore, the cause of apoptosis in the midguts is not simply due to a larger number of bacteria in the gut.

ROS production in the midgut following long-term ingestion of strains SK1-4 – Bacteria-derived uracil, which is secreted by pathogenic or opportunistic bacteria but not by commensal bacteria, acts as a signal to trigger the ROS production of DUOX through a G-protein-coupled receptor-mediated signaling pathway in the fly gut (16). ROS production in the midgut of gnotobiotic flies was examined after 18 days ingestion, using a fluorescent probe, CellROX green. The signal intensity of CellROX induced by ROS

production was measured quantitatively by a fluorescent cell imager. ROS production was statistically greater in the midgut of gnotobiotic flies that co-ingested SK4 and SK1 compared with that of gnotobiotic flies that mono-ingested SK4 (Fig. 8A). Interestingly, gnotobiotic flies that co-ingested SK4 and SK2 also exhibited high ROS production in the midgut (Fig. 8A). To confirm that ROS production was induced by co-ingestion of SK4 and SK1 or SK2, uracil-sensitive *Drosophila* S2 cells were treated with microbial extracts derived from mono- or co-incubated bacterial strains, as described in “EXPERIMENTAL PROCEDURES”. ROS production in S2 cells was examined using another fluorescent probe, 2', 7'-dichlorofluorescein-diacetate (DCF-DA). The number of fluorescence-positive cells was greater in S2 cells treated with the extract derived from co-incubated SK4 and SK1 or SK2, but not with the extracts derived from mono-incubated SK4, SK1, or SK2 (Fig. 8B).

Expression of IMD-AMP genes in gnotobiotic flies that mono- or co-ingested strains SK1-4 – TG-RNAi enhances the expression of IMD-AMP genes such as Cecropin A1 and Diptericin (23) (Fig. 2D). Here we examined the expression of these genes in gnotobiotic flies that mono- or co-ingested strains SK1-4 (Fig. 9). Unexpectedly, expression of both genes was markedly induced in gnotobiotic flies that co-ingested SK4 and SK2, but not gnotobiotic flies that co-ingested SK4 and SK1 or mono-ingested SK4. These findings suggest that the release of microbe-derived elicitors, peptidoglycans, to induce the expression of IMD-AMP genes was suppressed in the midgut in gnotobiotic flies that co-ingested SK4 and SK1 or mono-ingested SK4.

DISCUSSION

In the present study, 16S rDNA sequencing analysis and characterization of bacteria isolated from the gut revealed that microbiota comprising the single dominant genus of *Acetobacter* in non-*TG*-RNAi flies was shifted to that comprising the two dominant genera of *Acetobacter* and *Providencia* in *TG*-RNAi flies, leading to gut dysbiosis (Figs. 2A and 2B). Four bacterial strains, including *Acetobacter persici* SK1, *Acetobacter indonesiensis* SK2, *Lactobacillus pentosus* SK3, and *Providencia rettgeri* SK4, were isolated from the midgut of *TG*-RNAi flies. SK1 and SK3 were also isolated from the midgut of non-*TG*-RNAi flies. *Acetobacter*-dominated gut microbiota of *Drosophila* has been reported, and multiple factors could contribute to the establishment of the composition of microbiota, such as environmental circumstances, compatibility of bacteria, and transmission of bacteria from mother flies to their offspring (28, 30, 36). SK1 exhibited the strongest resistance against IMD-AMPs, including Cecropin A1 and Diptericin, and ROS, compared to the other three isolated bacteria (Figs. 3 and 4 and Tables 4 and 6), which could explain why the genus *Acetobacter* is dominant in non-*TG*-RNAi flies. Why the genus *Providencia* becomes another dominant genus in *TG*-RNAi flies, however, remains unclear, because SK4 exhibited very low resistance against Cecropin A1 with an IC_{50} value of 0.07 $\mu\text{g/mL}$, similar to the established bacteria *P. alcalifaciens* JCM 1673T with an IC_{50} of 0.05 $\mu\text{g/mL}$ (Table 4). In humans, *P. rettgeri* and *P. alcalifaciens* are opportunistic pathogens known to cause diarrhea (37). The resistance of strains SK1-4 against IMD-AMPs in *in vitro* assays could not explain the shift of microbiota in the gut in *TG*-RNAi flies. Interestingly, gene expression of IMD-AMPs was significantly suppressed in gnotobiotic flies that

co-ingested SK4 and SK1 or mono-ingested SK4 compared with that of gnotobiotic flies that co-ingested SK4 and SK2 (Fig. 9). It is possible that SK4 belonging to the opportunistic species *P. rettgeri* displays a cryptic defense mechanism against IMD-AMP gene expression depending on the environmental conditions in the midgut, but not in the *in vitro* culture conditions. SK4 exhibited much higher resistance to ROS than *P. alcalifaciens* JCM 1673T (Table 6). According to a septic injury model in *Drosophila*, *P. rettgeri* Dmel and *P. alcalifaciens* Dmel are moderately and highly virulent pathogens, respectively (38, 39), suggesting that SK4 becomes a virulent opportunistic bacterial strain in the fly gut.

In addition to the shift in the gut microbiota, 10-day-old *TG*-RNAi flies retained a higher bacterial load in the gut than 10-day-old non-*TG*-RNAi flies (Fig. 2C). We previously reported that systemic *TG*-RNAi causes a peritrophic matrix defect that allows for the penetration of dextran beads from the gut lumen into the ectoperitrophic space (23), and that *TG*-catalyzed crosslinking of peritrophic matrix protein is important for protection against pathogenic bacteria (40). The peritrophic matrix in the fly gut is a non-cellular sieve-like structure that lines the midgut epithelium and provides protection from food particles and enteric pathogens (10, 41), and therefore, the defect in the peritrophic matrix by *TG*-RNAi is a possible cause of the high bacterial load in *TG*-RNAi flies.

One of the important findings in this study is that gnotobiotic flies that co-ingested SK4 and SK1 had a short lifespan, but not gnotobiotic flies that mono-ingested each of the strains SK1-4 (Fig. 6A). In *Drosophila*, ingestion of pathogenic bacteria promotes excess generation of ROS to cause apoptosis, leading to a short lifespan (16). In gnotobiotic flies that co-ingested SK4 and SK1, the percentage of

TUNEL-positive guts and ROS production in the midgut were both statistically significant, but not in flies that mono-ingested SK4 (Figs. 7B and 8A). ROS production was also observed in S2 cells by adding the microbial extract derived from co-incubated SK4 and SK1, but not in the flies that mono-ingested SK4 or SK1 (Fig. 8B). These findings suggest that microbiota comprising the two dominant bacteria of the genus *Acetobacter* and *Providencia* in *TG*-RNAi flies may produce ROS, resulting in a short life span. Interestingly, gnotobiotic flies that co-ingested SK4 and SK2 exhibited significant ROS production in the midgut (Fig. 8A), and ROS production was also induced in S2 cells by treatment with microbial extract derived from co-incubated SK4 and SK2 (Fig. 8B). Gnotobiotic flies that co-ingested SK4 and SK2, however, exhibited no significant apoptosis of the midgut cells (Fig. 7) and did not have a significant short lifespan (Fig. 6A). To our knowledge, uracil is the only metabolite to trigger DUOX-dependent ROS production and it is released from pathobionts, not commensal bacteria (16,42), suggesting that uracil is secreted from the opportunistic strain *P. rettgeri* SK4 in the midgut of gnotobiotic flies that co-ingested SK4 and SK1 or SK2. In gnotobiotic flies that co-ingested SK4 and SK1, an additional unknown factor(s) may be required to cause midgut apoptosis, leading to a short lifespan.

EXPERIMENTAL PROCEDURES

Fly stocks – Flies were maintained at 25°C on standard *Drosophila* medium (% w/v): dry yeast (Oriental Yeast, Japan), 3.2; corn flour (GABAN, Japan), 3.2; glucose (Nacalai Tesque, Japan), 8.0; agar (Nacalai Tesque), 0.64; propionic acid (Nacalai Tesque), 0.24; and methyl *p*-hydroxybenzoate (Wako, Japan), 0.04. *Da-GAL4* and *w¹¹¹⁸* were obtained from the Bloomington Stock Center (Bloomington, IN, USA). *UAS-TG IR* flies were obtained from the National Institute of Genetics (Mishima, Japan). To obtain the *TG*-RNAi flies, *Da-GAL4* flies were crossed with *UAS-TG IR* flies, and to obtain the non-*TG*-RNAi flies, *Da-GAL4* flies were crossed with *w¹¹¹⁸* flies, as described previously (22). The fly strain *Rel^{E20}* was described previously (43).

Bacterial strains – *P. alcalifaciens* JCM 1673T and *P. azotoformans* IAM 1603 (JCM 2777) were obtained from the Japan Collection of Microorganisms, RIKEN BRC, participating in the National BioResource Project of the MEXT, Japan. *Ecc15* 2141 (44) was provided by S. Kurata at Tohoku University (Sendai, Japan). *G. morbifer* G707T, *C. intestini* A911T, *A. pomorum*, *L. brevis* EW, and *L. plantarum* WJL (24) were provided by W.-J. Lee at Seoul National University (Seoul, Korea).

Bacterial 16S rDNA analysis – Genomic DNAs from midguts of 0.5- and 10-day-old *TG*-RNAi (*Da>TG IR*) or non-*TG*-RNAi (*Da>+*) flies maintained under conventional rearing conditions were extracted using NucleoSpin® Tissue XS (MACHEREY-NAGEL GmbH & Co. KG, Germany). PCR amplification was performed for each sample with Tks Gflex™ DNA Polymerase (Takara Bio, Japan) using the following primers (45): forward primer, 515F 5'-AAT GAT ACG GCG ACC ACC GAG ATC

TAC ACT ATG GTA ATT GTG TGC CAG CMG CCG CGG TAA-3'; reverse primer, 806R 5'-CAA GCA GAA GAC GGC ATA CGA GAT XXX XXX XXX XXX AGT CAG TCA GCC GGA CTA CHV GGG TWT CTA AT-3'. The X-repeated sequence shows the Golay barcode (46). Cycling conditions were 1 min at 94°C, followed by 28 cycles of 10 s at 98°C, 15 s at 60°C, and 15 s at 68°C, and 5 min at 68°C at the final elongation step. PCR products were quantified by an Agilent 2100 Bioanalyzer (Agilent Technologies, USA) and then sequenced using an Illumina MiSeq sequencer (150 base-pair paired-end reads of the V4 region of the 16S rDNA) at Takara Bio. A total of 24,437,440 reads (2,500,000 ± 350,000 reads per sample) were obtained, and quality filtering, removal of chimeras, and de-noising were performed by CD-HIT-OTU 0.01 (<http://weizhong-lab.ucsd.edu/cd-hit-otu/>) (47) with default parameters. Sequences from Read 1 and Read 2 were clustered into operational taxonomic units (OTUs) at 97% identity using the CD-HIT-OTU pipeline, and then the sequences were taxonomically classified down to the genus level with the EzTaxon server (48).

Bacteria contain multiple heterogeneous 16S rRNA genes in their genomes, and the gene copy number information was obtained from the rRNA Operon Copy Number Database (*rrnDB*) (<http://rrndb.cme.msu.edu>). To estimate the effective number of reads, read count data of the next-generation sequencing were corrected using representative copy numbers of the corresponding genera, five copies for *Acetobacter* and seven copies for *Providencia*. The copy number of genus *Lactobacillus* varies from one to nine depending on the species, and the median number of the gene copies (5 copies) was used.

Quantitative PCR – To quantify the number of bacteria, 16S rRNA bacteria-specific oligonucleotide primers, HDA1 (5'- ACT CCT ACG GGA GGC AGC AGT -3') and HDA2 (5'- GTA TTA CCG CGG CTG CTG GCA C -3'), were used (23). The theoretical coverage rate of the HDA1-HDA2 primer set at the genus level was evaluated to be 99.4% for *Acetobacter*, 98.3% for *Providencia*, and 96.1% for *Lactobacillus*, using the TestPrime 1.0 program (<http://www.arb-silva.de/search/testprime/>). Standard calibration curves were generated using 10-fold serial dilutions of a plasmid containing a segment of the *rp49* or 16S rRNA genes. Genomic DNA was extracted from the midguts of 0.5- and 10-day-old non-*TG*-RNAi and *TG*-RNAi flies (4 guts per sample) by phenol/chloroform extraction, and used as templates. The number of gut bacteria was estimated after correction using the representative copy numbers, as described under “*Bacterial 16S rDNA analysis*”, and then normalized to the amount of genomic *rp49*, and estimated per gut. To quantify the copy number of *Cecropin A1* and *Diptericin*, total RNA from conventionally reared adult midguts or germ-free adult midguts following 18 days ingestion were extracted with RNAiso (Takara Bio, Japan) and treated with deoxyribonuclease I, and then total RNA (400~450 ng) was used as template for reverse transcription using SuperScript III (Life Technologies Co. Ltd., USA). Absolute copy numbers analyzed for *Cecropin A1* and *Diptericin* were normalized to absolute control *rp49* mRNA copy numbers. Standard calibration curves were generated using 10-fold serial dilutions of a plasmid containing a segment of the *rp49*, *Cecropin A1*, and *Diptericin*. The set of PCR primers was previously described (23). All qPCR was performed with FastStart Essential DNA Green Master (Roche, USA), and the reactions were performed on a LightCycler Nano (Roche,

USA).

Isolation of gut microbes – To obtain strains belonging to the genera *Acetobacter* and *Lactobacillus*, homogenates of midguts (1-2 guts dissected from adult 10- to 12-day-old *TG*-RNAi or non-*TG*-RNAi flies) were plated on Hestrin-Schramm medium plates containing 2.0% glucose, 0.5% bacto peptone (Difco, USA), 0.5% yeast extract (Difco, USA), 0.68% Na₂HPO₄·12H₂O, 0.15% citric acid monohydrate, and 1.5% agar adjusted to pH5.0 with 1 M CH₃COOH (49), and incubated for 2 days at 30°C. To obtain strains belonging the genera *Providencia* species, homogenates of midguts (1-2 guts dissected from adult 10- to 12-day-old *TG*-RNAi or non-*TG*-RNAi flies) were plated on nutrient agar medium plates containing 5.0% bacto peptone, 3.0% beef extract (MP Biomedicals, USA), 1.5% agar, 0.05% phenol red, 0.04% 2,3,5-triphenyl tetrazolium chloride (50, 51), and incubated for 16 h at 37°C. Bacterial colonies (24 and 57 colonies for non-*TG*-RNAi and *TG*-RNAi flies, respectively) were randomly isolated and sequenced. Bacterial 16S rDNA was sequenced using 16S universal primers, 8FE (5'-AGA GTT TGA TCM TGG CTC AG-3') and 1492R (5'-GGM TAG CTT GTT ACG ACT T-3'). The similarity of the sequenced data was determined using an EzTaxon server (48).

Antimicrobial activity – Peptide synthesis of Cecropin A1 and Diptericin was outsourced to Genenet Co., Ltd, Japan. The peptide sequence of Cecropin A1 is GWLKK IGKKI ERVGQ HTRDA TIQGL GIAQQ AANVA ATAR-NH₂ (39 residues), and the peptide sequence of Diptericin is DDMTM KPTPP PQYPL NLQGG GGGQS GDGFG FAVQG HQKVW TSDNG RHEIG LNGGY GQHLG GPYGN SEPSW KVGST YTYRF PNF-NH₂ (83 residues). Antimicrobial activities were assayed as described

previously (52). In brief, bacteria were grown under the following conditions: Hestrin-Schramm medium for *Acetobacter* and *Lactobacillus* isolated from the gut and incubated for 2 days at 30°C. *G. morbifer* G707T, *C. intestini* A911T, and *A. pomorum* were cultured for 2 days at 30°C in mannitol broth containing 2.5 % mannitol (Nacalai Tesque, Japan), 0.3% bacto peptone, and 0.5% yeast extract (53). *L. brevis* EW and *L. plantarum* WJL were cultured for 2 days at 30°C in MRS broth containing 2.0% glucose, 1.0% bacto tryptone (Difco, USA), 1.0% beef extract, 0.5% yeast extract, 0.5% CH₃COONa, 0.2% K₂HPO₄, 0.2% di-ammonium hydrogen citrate, 0.1% polysorbate 80, 0.02% MgSO₄·7H₂O, and 0.005% MnSO₄·5H₂O (54). *Providencia*, *E. coli* K12, *Ecc15*, and *P. azotoformans* IAM 1603 were cultured in Luria-Bertani medium and incubated 16 h at 37°C. Bacteria collected by centrifugation were washed three times with PBS containing 8.0% NaCl, 0.2% KCl, 2.9% Na₂HPO₄·12H₂O, and 0.2% KH₂PO₄, and suspended in 10 mM HEPES-NaOH, pH 7.5. Then, 50 µL of antimicrobial peptide solution in 10 mM HEPES-NaOH, pH 7.5, was added to 450 µL of the bacterial suspensions and the mixtures were incubated at 37°C for 1 h and plated onto three agar plates (100 µL each). Each plate was incubated at either 30°C for 2 days or 37°C for 16 h.

HOCl resistance assay – Hypochlorous acid (HOCl) resistance assays were performed as described previously (55). The concentration of available chlorine was measured using *N,N*-diethylphenylenediamine (56). In brief, bacteria collected by centrifugation were washed three times with PBS, and suspended in 10 mM HEPES-NaOH, pH 7.5. Then, 50 µL of the freshly prepared NaOCl solution in 10 mM HEPES-NaOH, pH 7.5, containing 150 µg/L or 500 µg/L available chlorine was added

to 450 μL of the bacteria suspensions and the mixture was incubated at 37°C for 40 min. To stop the reaction, aliquots (5 μL each) of the incubated samples were transferred to 495 μL of PBS, and plated onto three agar plates (100 μL each).

Bacterial ingestion and survival experiments – Survival rate experiments were performed using conventionally reared, germ-free, and long-term ingested germ-free flies. Germ-free flies were maintained as described previously (23). Bacterial contamination in germ-free flies was checked by PCR analysis using the 16S rDNA universal primers (8FE and 1492R). For long-term ingestion experiments, 1- to 3-day-old germ-free flies were transferred to a fresh vial containing in total 4.0×10^9 cells isolated bacteria or a mixture of the isolated bacteria (*Providencia/Acetobacter* ratio was 1:1), and then transferred to a fresh vial containing 4.0×10^9 cells of bacteria every 3 days.

Bacterial colonization ability in the midgut of Drosophila – To examine transient colonization of flies with bacteria, 3- to 5-day-old adult germ-free flies were transferred to a fresh vial containing 4.0×10^9 bacterial cells in 5 % sucrose solution for 24 h, and then transferred into sterile vials containing sterile food. After 5 h of incubation, midguts were dissected into three parts and homogenized in 100 μL sterile PBS. To examine the colonization ability in flies after long-term ingestion of bacteria, the midguts were dissected after 15 and 25 days ingestion and homogenized in 100 μL sterile PBS. The homogenates were 2-, 20-, 200-, or 2000-fold diluted with sterile PBS, then 5 μL aliquots of the homogenates were spotted onto agar plates and incubated under the following conditions: Hestrin-Schramm medium plates for flies that mono-ingested SK1, SK2, and SK3, and then incubated for 2 days at 30°C; Luria-Bertani medium

plates for flies that mono-ingested SK4 and then incubated for 16 h at 37°C. For flies that co-ingested the bacteria, 5 µL aliquots of the serial dilutions were spotted onto Hestrin-Schramm medium plates and incubated for 2 days at 30°C, and a second 5 µL aliquot of each dilution was spotted onto Luria-Bertani medium plates and incubated for 16 h at 37°C. The number of CFUs in two or three selected spots was counted and the average CFUs were calculated.

TUNEL imaging analysis – For detection of apoptosis in midgut cells, the TUNEL method was performed using an In Situ Cell Death Detection Kit, Fluorescein (Roche, USA), as previously described (23). The guts were stained with DAPI (1:2,000, Dojindo Molecular Technologies, Japan). Midguts were dissected from adult flies following 18 days ingestion. The samples were analyzed with a ZOE™ Fluorescent Cell Imager (BIO-RAD, USA). Each experiment was repeated at least three times with samples dissected on different dates.

ROS measurement – To measure ROS production *in vivo*, midguts were dissected from adult flies following 18 days ingestion in the presence of 20 mM *N*-acetyl cysteine (Sigma, USA). Midguts were incubated with 5 µM CellROX (Molecular Probes, USA) for 30 min at 37°C, and then fixed by 4% paraformaldehyde. As a positive control for oxidative stress, the ROS inducer paraquat (Nacalai Tesque, Japan) was fed to adult germ-free flies for 3 h prior to dissection. As a negative control, midguts were dissected from 1- to 2-day-old germ-free flies. After mounting with 70% glycerol, samples were analyzed with a ZOE™ Fluorescent Cell Imager. The resulting signal intensity was measured by ImageJ (National Institute of Health, USA) and normalized to the average of negative control gut signal intensity. Each

experiment was repeated at least three times with samples dissected on different dates. To measure ROS production *in vitro*, S2 cells were maintained in Insect-XPRESS protein-free insect cell medium (Lonza, Switzerland) at 27°C. Soluble microbial extracts was prepared as described previously (57). In brief, bacteria were grown under the following conditions: Hestrin-Schramm medium was used for the genus *Acetobacter* and the plates were incubated for 2 days at 30°C. Luria-Bertani medium was used for the genus *Providencia* and the plates were incubated for 16 h at 37°C. After washing with PBS, bacteria were adjusted to 7.0×10^9 cells or a mixture of bacteria (*Providencia/Acetobacter* ratio was 1.0) in 5 mL of PBS buffer. The bacterial solutions were incubated for 1 h at 30°C, 200 rpm, and then collected by centrifugation. S2 cells were treated with 10 µg/mL of soluble microbial extract in the medium for 1 h. Uracil at 20 nM was added as a positive control to produce ROS. The cells were stained with Hoechst 33342 (1:1,000, Dojindo Molecular Technologies, Japan) and 2 µM DCF-DA (Sigma, USA). After washing with PBS, the fluorescent signal was observed using a ZOE Fluorescent Cell Imager. From these pictures, Hoechst 33342-stained nuclei, representing all cells, were randomly defined and the number of DCF-DA-positive cells, representing ROS-positive cells, was determined.

REFERENCES

1. Guinane, C. M., and Cotter, P. D. (2013) Role of the gut microbiota in health and chronic gastrointestinal disease: understanding a hidden metabolic organ. *Ther. Adv. Gastroenterol.* **6**, 295–308
2. Lee, W.-J., and Hase, K. (2014) Gut microbiota-generated metabolites in animal health and disease. *Nat. Chem. Biol.* **10**, 416–424
3. Lee, K.-A., and Lee, W.-J. (2014) Drosophila as a model for intestinal dysbiosis and chronic inflammatory diseases. *Dev. Comp. Immunol.* **42**, 102–110
4. Ma, D., Storelli, G., Mitchell, M., and Leulier, F. (2015) Studying host-microbiota mutualism in Drosophila: Harnessing the power of gnotobiotic flies. *Biomed. J.* **38**, 285
5. Ren, C., Webster, P., Finkel, S. E., and Tower, J. (2007) Increased internal and external bacterial load during Drosophila aging without life-span trade-off. *Cell Metab.* **6**, 144–152
6. Cox, C. R., and Gilmore, M. S. (2007) Native microbial colonization of Drosophila melanogaster and its use as a model of Enterococcus faecalis pathogenesis. *Infect. Immun.* **75**, 1565–1576
7. Wong, C. N. A., Ng, P., and Douglas, A. E. (2011) Low-diversity bacterial community in the gut of the fruitfly Drosophila melanogaster. *Environ. Microbiol.* **13**, 1889–1900
8. Buchon, N., Broderick, N. A., and Lemaitre, B. (2013) Gut homeostasis in a microbial world: insights from Drosophila melanogaster. *Nat. Rev. Microbiol.* **11**, 615–626
9. Buchon, N., Osman, D., David, F. P. A., Yu Fang, H., Boquete, J.-P., Deplancke, B., and Lemaitre, B. (2013) Morphological and molecular characterization of adult midgut compartmentalization in Drosophila. *Cell Rep.* **3**, 1725–1738

10. Kuraishi, T., Hori, A., and Kurata, S. (2013) Host-microbe interactions in the gut of *Drosophila melanogaster*. *Front. Physiol.* **4**, 375
11. Kim, S.-H., and Lee, W.-J. (2014) Role of DUOX in gut inflammation: lessons from *Drosophila* model of gut-microbiota interactions. *Front. Cell. Infect. Microbiol.* 10.3389/fcimb.2013.00116
12. Ryu, J.-H., Ha, E.-M., and Lee, W.-J. (2010) Innate immunity and gut-microbe mutualism in *Drosophila*. *Dev. Comp. Immunol.* **34**, 369–376
13. Ryu, J.-H., Ha, E.-M., Oh, C.-T., Seol, J.-H., Brey, P. T., Jin, I., Lee, D. G., Kim, J., Lee, D., and Lee, W.-J. (2006) An essential complementary role of NF - κ B pathway to microbicidal oxidants in *Drosophila* gut immunity. *EMBO J.* **25**, 3693–3701
14. Ha, E.-M., Oh, C.-T., Ryu, J.-H., Bae, Y.-S., Kang, S.-W., Jang, I., Brey, P. T., and Lee, W.-J. (2005) An antioxidant system required for host protection against gut Infection in *Drosophila*. *Dev. Cell.* **8**, 125–132
15. Capo, F., Charroux, B., and Royet, J. (2016) Bacteria sensing mechanisms in *Drosophila* gut: Local and systemic consequences. *Dev. Comp. Immunol.* **64**, 11–21
16. Lee, K.-A., Kim, S.-H., Kim, E.-K., Ha, E.-M., You, H., Kim, B., Kim, M.-J., Kwon, Y., Ryu, J.-H., and Lee, W.-J. (2013) Bacterial-derived uracil as a modulator of mucosal immunity and gut-microbe homeostasis in *Drosophila*. *Cell.* **153**, 797–811
17. Lorand, L., and Graham, R. M. (2003) Transglutaminases: crosslinking enzymes with pleiotropic functions. *Nat. Rev. Mol. Cell Biol.* **4**, 140–156
18. Beninati, S., and Piacentini, M. (2004) The Transglutaminase family: an overview: Minireview article. *Amino Acids.* **26**, 367–372

19. Kopáček, P., Hall, M., and Söderhäll, K. (1993) Characterization of a clotting protein, isolated from plasma of the freshwater crayfish *Pacifastacus leniusculus*. *Eur. J. Biochem.* **213**, 591–597
20. Theopold, U., Schmidt, O., Söderhäll, K., and Dushay, M. S. (2004) Coagulation in arthropods: defence, wound closure and healing. *Trends Immunol.* **25**, 289–294
21. Kawabata, S. (2010) Immunocompetent molecules and their response network in horseshoe crabs. in *Invertebrate Immunity* (Söderhäll, K. ed), pp. 122–136, Springer Science + Business Media, New York
22. Shibata, T., Ariki, S., Shinzawa, N., Miyaji, R., Suyama, H., Sako, M., Inomata, N., Koshiba, T., Kanuka, H., and Kawabata, S. (2010) Protein crosslinking by Transglutaminase controls cuticle morphogenesis in *Drosophila*. *PLoS ONE.* **5**, e13477
23. Shibata, T., Sekihara, S., Fujikawa, T., Miyaji, R., Maki, K., Ishihara, T., Koshiba, T., and Kawabata, S. (2013) Transglutaminase-catalyzed protein-protein cross-linking suppresses the activity of the NF- κ B-like transcription factor Relish. *Sci. Signal.* **6**, ra61
24. Ryu, J.-H., Kim, S.-H., Lee, H.-Y., Bai, J. Y., Nam, Y.-D., Bae, J.-W., Lee, D. G., Shin, S. C., Ha, E.-M., and Lee, W.-J. (2008) Innate immune homeostasis by the homeobox gene *Caudal* and commensal-gut mutualism in *Drosophila*. *Science.* **319**, 777–782
25. Chandler, J. A., Jenna, M. L., Bhatnagar, S., Eisen, J. A., and Kopp, A. (2011) Bacterial communities of diverse *Drosophila* species: Ecological context of a host–microbe model system. *PLoS Genet.* **7**, e1002272
26. Blum, J. E., Fischer, C. N., Miles, J., and Handelsman, J. (2013) Frequent replenishment sustains the beneficial microbiome of *Drosophila melanogaster*. *mBio.* **4**, e00860-13

27. Amir, A., Zeisel, A., Zuk, O., Elgart, M., Stern, S., Shamir, O., Turnbaugh, P. J., Soen, Y., and Shental, N. (2013) High-resolution microbial community reconstruction by integrating short reads from multiple 16S rRNA regions. *Nucleic Acids Res.* **41**, e205
28. Staubach, F., Baines, J. F., Künzel, S., Bik, E. M., and Petrov, D. A. (2013) Host species and environmental effects on bacterial communities associated with *Drosophila* in the laboratory and in the natural environment. *PLoS ONE*. **8**, e70749
29. Broderick, N. A., Buchon, N., and Lemaitre, B. (2014) Microbiota-induced changes in *Drosophila melanogaster* host gene expression and gut morphology. *mBio*. **5**, e01117-14
30. Wong, A. C.-N., Luo, Y., Jing, X., Franzenburg, S., Bost, A., and Douglas, A. E. (2015) The host as the driver of the microbiota in the gut and external environment of *Drosophila melanogaster*. *Appl. Environ. Microbiol.* **81**, 6232–6240
31. Hertig, M., and Wolbach, S. B. (1924) Studies on Rickettsia-like micro-organisms in insects. *J. Med. Res.* **44**, 329–374.7
32. Ha, E.-M., Oh, C.-T., Bae, Y. S., and Lee, W.-J. (2005) A direct role for Dual oxidase in *Drosophila* gut immunity. *Science*. **310**, 847–850
33. Macpherson, A. J., and Harris, N. L. (2004) Interactions between commensal intestinal bacteria and the immune system. *Nat. Rev. Immunol.* **4**, 478–485
34. Spasova, D. S., and Surh, C. D. (2014) Blowing on embers: Commensal microbiota and our immune system. *Front. Immunol.* 10.3389/fimmu.2014.00318
35. Shin, S. C., Kim, S.-H., You, H., Kim, B., Kim, A. C., Lee, K.-A., Yoon, J.-H., Ryu, J.-H., and Lee, W.-J. (2011) *Drosophila* microbiome modulates host developmental and metabolic

- homeostasis via insulin signaling. *Science*. **334**, 670–674
36. Erkosar, B., and Leulier, F. (2014) Transient adult microbiota, gut homeostasis and longevity: Novel insights from the *Drosophila* model. *FEBS Lett*. **588**, 4250–4257
 37. Yoh, M., Matsuyama, J., Ohnishi, M., Takagi, K., Miyagi, H., Mori, K., Park, K.-S., Ono, T., and Honda, T. (2005) Importance of *Providencia* species as a major cause of travellers' diarrhoea. *J. Med. Microbiol*. **54**, 1077–1082
 38. Galac, M. R., and Lazzaro, B. P. (2011) Comparative pathology of bacteria in the genus *Providencia* to a natural host, *Drosophila melanogaster*. *Microbes Infect*. **13**, 673–683
 39. Chambers, M. C., Jacobson, E., Khalil, S., and Lazzaro, B. P. (2014) Thorax injury lowers resistance to infection in *Drosophila melanogaster*. *Infect. Immun*. **82**, 4380–4389
 40. Shibata, T., Maki, K., Hadano, J., Fujikawa, T., Kitazaki, K., Koshiba, T., and Kawabata, S. (2015) Crosslinking of a peritrophic matrix protein protects gut epithelia from bacterial exotoxins. *PLoS Pathog*. **11**, e1005244
 41. Lehane, M. J. (1997) Peritrophic matrix structure and function. *Annu. Rev. Entomol*. **42**, 525–550
 42. Lee, K.-A., Kim, B., Bhin, J., Kim, D. H., You, H., Kim, E.-K., Kim, S.-H., Ryu, J.-H., Hwang, D., and Lee, W.-J. (2015) Bacterial uracil modulates *Drosophila* DUOX-dependent gut immunity via Hedgehog-induced signaling endosomes. *Cell Host Microbe*. **17**, 191–204
 43. Hedengren, M., Bengt Åsling, Dushay, M. S., Ando, I., Ekengren, S., Wihlborg, M., and Hultmark, D. (1999) Relish, a central factor in the control of humoral but not cellular immunity in *Drosophila*. *Mol. Cell*. **4**, 827–837
 44. Basset, A., Khush, R. S., Braun, A., Gardan, L., Boccard, F., Hoffmann, J. A., and Lemaitre, B.

- (2000) The phytopathogenic bacteria *Erwinia carotovora* infects *Drosophila* and activates an immune response. *Proc. Natl. Acad. Sci. U. S. A.* **97**, 3376–3381
45. Chassaing, B., Koren, O., Goodrich, J. K., Poole, A. C., Srinivasan, S., Ley, R. E., and Gewirtz, A. T. (2015) Dietary emulsifiers impact the mouse gut microbiota promoting colitis and metabolic syndrome. *Nature.* **519**, 92–96
46. Caporaso, J. G., Lauber, C. L., Walters, W. A., Berg-Lyons, D., Huntley, J., Fierer, N., Owens, S. M., Betley, J., Fraser, L., Bauer, M., Gormley, N., Gilbert, J. A., Smith, G., and Knight, R. (2012) Ultra-high-throughput microbial community analysis on the Illumina HiSeq and MiSeq platforms. *ISME J.* **6**, 1621–1624
47. Li, W., Fu, L., Niu, B., Wu, S., and Wooley, J. (2012) Ultrafast clustering algorithms for metagenomic sequence analysis. *Brief. Bioinform.* 10.1093/bib/bbs035
48. Chun, J., Lee, J.-H., Jung, Y., Kim, M., Kim, S., Kim, B. K., and Lim, Y.-W. (2007) EzTaxon: a web-based tool for the identification of prokaryotes based on 16S ribosomal RNA gene sequences. *Int. J. Syst. Evol. Microbiol.* **57**, 2259–2261
49. Hestrin, S., and Schramm, M. (1954) Synthesis of cellulose by *Acetobacter xylinum*. 2. Preparation of freeze-dried cells capable of polymerizing glucose to cellulose. *Biochem. J.* **58**, 345–352
50. Somvanshi, V. S., Lang, E., Sträubler, B., Spröer, C., Schumann, P., Ganguly, S., Saxena, A. K., and Stackebrandt, E. (2006) *Providencia vermicola* sp. nov., isolated from infective juveniles of the entomopathogenic nematode *Steinernema thermophilum*. *Int. J. Syst. Evol. Microbiol.* **56**, 629–633

51. Senior, B. W. (1997) Media for the detection and recognition of the enteropathogen *Providencia alcalifaciens* in faeces. *J. Med. Microbiol.* **46**, 524–527
52. Kawabata, S., Nagayama, R., Hirata, M., Shigenaga, T., Agarwala, K. L., Saito, T., Cho, J., Nakajima, H., Takagi, T., and Iwanaga, S. (1996) Tachycitin, a small granular component in horseshoe crab hemocytes, is an antimicrobial protein with chitin-binding activity. *J. Biochem. (Tokyo)*. **120**, 1253–1260
53. American Society for Microbiology. Committee on Bacteriological Technic (1957) *Manual of microbiological methods*, McGraw-Hill, New York
54. De Man, J. C., Rogosa, M., and Sharpe, M. E. (1960) A medium for the cultivation of *Lactobacilli*. *J. Appl. Bacteriol.* **23**, 130–135
55. Fukuzaki, S., Urano, H., and Yamada, S. (2007) Effect of pH on the efficacy of sodium hypochlorite solution as cleaning and bactericidal agents. *J. Surf. Finish. Soc. Jpn.* **58**, 465–465
56. Urano, H., Ishikawa, H., and Fukuzaki, S. (2006) Involvement of radical species in inactivation of *Vibrio parahaemolyticus* in saline solutions by direct-current electric treatment. *J. Biosci. Bioeng.* **102**, 457–463
57. Ha, E.-M., Lee, K.-A., Park, S. H., Kim, S.-H., Nam, H.-J., Lee, H.-Y., Kang, D., and Lee, W.-J. (2009) Regulation of DUOX by the $G\alpha_q$ -phospholipase $C\beta$ - Ca^{2+} pathway in *Drosophila* gut immunity. *Dev. Cell.* **16**, 386–397

FIGURE LEGENDS

Fig. 1. Survival rates of non-*TG*-RNAi flies and *TG*-RNAi flies. The survival rates of conventionally reared non-*TG*-RNAi (*Da*>+, *n* = 59; closed circles) and *TG*-RNAi (*Da*>*TG* IR, *n* = 80; open circles) flies are shown. *P* values were calculated by the log-rank test. ****P* < 0.005.

Fig. 2. Gut flora of non-*TG*-RNAi flies and *TG*-RNAi flies. (A) Gut microbiota in 0.5-day-old flies. For non-*TG*-RNAi and *TG*-RNAi flies, 160 and 162 flies were analyzed, respectively. (B) Gut microbiota in 10-day-old flies. For non-*TG*-RNAi and *TG*-RNAi flies, 200 and 126 flies were analyzed, respectively. In all cases, the male/female ratio was 1.0. (C) Four midguts of 0.5-day-old or 10-day-old flies (male/female ratio was 1.0) were mixed into one tube and extracted 16S rDNA was analyzed by quantitative PCR. The bacterial loads are shown as 16S rDNA copies per midgut. The analysis was repeated four times. Closed circles, non-*TG*-RNAi; open circles, *TG*-RNAi. Bars indicate the means of four independent experiments. *P* values were calculated using Student's t-test. **P* < 0.05. (D) mRNA expression levels of *Cecropin A1* in the gut of 0.5-day-old and 10-day-old non-*TG*-RNAi, *TG*-RNAi, and *Relish* null (*Rel^{E20}*) flies. Results are shown as the *Cecropin A1*/*rp49* ratio. Values shown are means ± SEM (*n* = 2). *P* values were calculated by one-way ANOVA followed by the Bonferroni post hoc test. **P* < 0.05 and n.s, not significant.

Fig. 3. Bacterial colonization ability in fly midguts after transient ingestion of strains SK1-4. The bacterial strains were ingested by 3- to 5-day-old adult non-*TG*-RNAi and *TG*-RNAi flies for 24 h, and then the flies were transferred into sterile vials containing sterile food. After 5 h incubation, midguts

were removed and dissected into three regions: the anterior midgut (A), middle midgut (copper-cell region) (M), and posterior midgut (P). The three dissected parts were homogenized, spotted onto the strain-specific agar plates, and the resulting bacterial colonies were counted as described in “EXPERIMENTAL PROCEDURES”. Upper image shows a schematic image of the *Drosophila* midgut. Horizontal bars represent the median CFUs per fly for each ingestion group. Each denominator and numerator of the fractions shows the number of all guts used for the experiments and the number of guts with bacteria growing on agarose plates, respectively. *P* values were calculated by the non-parametric Mann–Whitney U test. **P* < 0.05 and n.s, not significant.

Fig. 4. Antimicrobial resistance of strains SK1-4 and established bacteria to Cecropin A1.

Inhibitory activity was measured after incubating bacteria in the presence of different concentrations of Cecropin A1 against strains SK1-4 and established bacteria. Values shown are means ± SEM (*n* =3).

The dashed line represents the half maximal inhibitory concentration (IC₅₀) of Cecropin A1.

Fig. 5. Antimicrobial resistance of strains SK1-4 and established bacteria to Diptericin.

Inhibitory activity was measured after incubating bacteria in the presence of different concentrations of Diptericin against strains SK1-4 and established bacteria. Values are shown as means ± SEM (*n* =3).

The dashed line represents the half maximal inhibitory concentration (IC₅₀) of Diptericin.

Fig. 6. Survival rates and bacterial colonization in the gut after long-term mono- or co-ingestions

of strains SK1-4. (A) Survival rates of *w¹¹¹⁸* flies after long-term mono- or co-ingestion. Ingestion

groups were as follows: crosses, PBS ($n = 40$); closed circles, SK1 ($n = 48$); open circles, SK2 ($n = 54$); closed triangles, SK3 ($n = 54$); open triangles, SK4 ($n = 54$); closed squares, mixture of SK1 and SK4 ($n = 54$); open squares, mixture of SK2 and SK4 ($n = 54$). P values were calculated with the log-rank test. $***P < 0.005$. (B) Bacterial colonization ability in *w¹¹¹⁸* germ-free flies after 15 and 25 days continuous mono-ingestion or co-ingestion. Box plots represent the interquartile range (boxes), the median (a horizontal line in each box), and whiskers extend towards the minimum and maximum values. Each denominator and numerator of the fractions shows the number of all guts used for the experiments and the number of guts with bacteria growing on agarose plates, respectively. P values were calculated by the non-parametric Mann–Whitney U test. $*P < 0.05$, $**P < 0.01$, $***P < 0.005$, and n.s, not significant.

Fig. 7. TUNEL assays in the midguts of gnotobiotic flies that mono- or co-ingested strains SK1-4.

(A) TUNEL staining of apoptotic cells in the fly midgut after 18 days continuous ingestion. Images show the copper cell region of the midgut. Arrowheads indicate representative TUNEL-positive cells. Green, TUNEL-positive cells; blue, DAPI nuclear stain; scale bar, 50 μm . (B) The percentage of guts showing apoptosis-positive signals were counted. The values shown are means \pm SEM ($n = 3$). P values were calculated by one-way ANOVA followed by the Bonferroni post hoc test. $*P < 0.05$ and n.s, not significant.

Fig. 8. ROS production in the midguts of gnotobiotic flies that mono- and co-ingested strains

SK1-4. (A) As a positive control for ROS production, flies ingested 5 mM paraquat. Fold-change in

mean gray value of CellROX signal intensity in the anterior midgut was evaluated and normalized to the negative control (average signal intensity of negative control was set to 1). Horizontal bars represent the median fold-change for each ingestion group with the fold-change value. Ingestion groups were as follows: paraquat ($n = 14$); PBS ($n = 36$); SK4 ($n = 38$); SK4+SK2 ($n = 46$); SK4+SK1 ($n = 61$). Statistical analysis of the differences between the five ingestion groups was performed using the non-parametric Kruskal-Wallis test followed by the Bonferroni post hoc test. $***P < 0.005$, $****P < 0.001$, and n.s, not significant. (B) ROS production in S2 cells treated with microbial extracts. The fold-change of DCF-DA-positive cell number was analyzed (1000 of S2 cells of each group). The values shown are the means \pm SEM ($n = 3$). P values were calculated by one-way ANOVA followed by the Bonferroni post hoc test. $**P < 0.01$, $***P < 0.005$, and n.s, not significant.

Fig. 9. Gene expression of IMD-AMPs in gnotobiotic flies that mono- and co-ingested strains SK1-4. Gene expression of *Cecropin A1* or *Diptericin* was analyzed by quantitative PCR in the fly midgut after 18 days of continuous ingestion. Results are shown as the *Cecropin A1/rp49* and *Diptericin /rp49* ratio. Values shown are means \pm SEM ($n = 3$). P values were calculated by one-way ANOVA followed by the Bonferroni post hoc test. $*P < 0.05$ and n.s, not significant.

TABLES

Table 1. Sequences of the V4 region of 16S rDNA clones obtained from the gut of non-TG-RNAi or TG-RNAi flies.

Genera identified	Sequences of the V4 region of the 16S rDNA clones
<i>Acetobacter</i>	5'-tacgaaggggctagcgttgctcggaatgactgggcgtaaagggcgtgtaggcggttgacagtagatgtgaaatccccgggcttaacctgggagctgcatttaagacgtgcagactagagtgtgagagagggttggaa ttccagtgtagagggtgaaattcgtagatattgggaagaacaccgggtggcgaaggcggcaacctggctcatg actgacgtgaggcgcgaaagcgtggggagcaaacagg-3'
<i>Lactobacillus</i>	5'-tacgtaggtggcaagcgttgccggatttattggcgtaaagcgagcgcaggcggtttttaagtctgatgt gaaagccttcggctcaaccgaagaagtgcacggaactgggaaacttgagtgcagaagaggacagtggaactccatgtgtagcgggtgaaatgcgtagatatatggaagaacaccagtggcgaaggcggctgtctgtctgtaa ctgacgtgaggctcgaagtatgggtagcaaacagg-3'
<i>Providencia</i>	5'-tacggagggtgcaagcgttaatcggaaactgggcgtaaagcgacgcaggcgggtgattaagtagatgtgaaatccccgggcttaacctgggaatggcatctaagactggtcagctagagtctttagagggggtagaa ttccatgtgtagcgggtgaaatgcgtagagatgtggaggaataccgggtggcgaaggcggccccctggacaaa gactgacgtcaggtgcgaaagcgtggggagcaaacagg-3'
<i>Wolbachia</i>	5'-tacggagagggctagcgttattcggaaattattggcgtaaagggcgcgtaggcggattagtaagttaaa gtgaaatccaaggctcaaccttgaattgcttttaaactgctaacttagagattgaaagaggatagaggaatt cctagtgtagagggtgaaattcgtaaatattaggaggaacaccagtggcgaaggcgtctatctggttcaaatctg acgctgaggcgcgaaaggcgtggggagcaaacagg-3'

Table 2. Bacteria highly matched with the sequences of the V4 region of the 16S rDNA clones.

Genera identified	Highly matched bacterial strains	Identity (%)
<i>Acetobacter</i>	<i>Acetobacter persici</i> T-120T	99.6
	<i>A. farinalis</i> G360-1T	99.2
	<i>A. cerevisiae</i> LMG 1625T	98.8
	<i>A. indonesiensis</i> NRIC 0313T	98.0
<i>Lactobacillus</i>	<i>Lactobacillus pentosus</i> JCM 1558T	100
	<i>L. fabifermentans</i> DSM 21115T	100
	<i>L. paraplantarum</i> DSM 10667T	100
	<i>L. plantarum subsp. plantarum</i> ATCC 14917T	100
<i>Providencia</i>	<i>Providencia rettgeri</i> Dmel1 ^{a)}	100
	<i>P. alcalifaciens</i> DSM 30120T	100
	<i>P. rustigianii</i> DSM 4541T	100
	<i>P. vermicola</i> OP1T	100
	<i>P. sneebia</i> DSM 19967T	100
<i>Wolbachia</i>	<i>Wolbachia pipientis</i> ωPip	95.7

a) reference (38)

Table 3. The closest bacterium matching the 16S rDNA sequence of the bacterium isolated from the gut of non-TG-RNAi or TG-RNAi flies.

Isolated bacterial strains	Closest bacterial strain	Identity (%)
SK1 (LC037412)	<i>A. persici</i> T-120T (BAJW01000143)	99.7
SK2 (LC037413)	<i>A. indonesiensis</i> NRIC 0313T (AB032356)	99.6
SK3 (LC037414)	<i>L. pentosus</i> JCM 1558T (D79211)	100
SK4 (LC079061)	<i>P. rettgeri</i> DSM 4542T (AM040492)	99.8

GenBank accession numbers are shown in parentheses.

Table 4. IC₅₀ of Cecropin A1 and Diptericin to strains SK1-4 and established bacteria.

Bacterial strains	Cecropin A1	Diptericin
		- IC ₅₀ (µg/mL) -
<i>A. persici</i> SK1	> 10	No inhibition
<i>A. indonesiensis</i> SK2	0.22	> 20
<i>L. pentosus</i> SK3	0.35	No inhibition
<i>P. rettgeri</i> SK4	0.07	> 100
<i>Ecc15</i> 2141	0.05	1.0
<i>P. azotoformans</i> IAM1603	0.06	6.0
<i>E. coli</i> K12	0.06	3.0
<i>P. alcalifaciens</i> JCM1673T	0.05	> 100

Table 5. Antimicrobial resistance of the gut strains isolated by Ryu et al (24).

Bacterial strains	Cecropin A1 at 1µg/mL	Diptericin at 10µg/mL
	- Growth inhibition (%) -	
<i>Gluconobacter morbifer</i> G707T	80±0.6	20±5.9
<i>Commensalibacter intestini</i> A911T	8.9±8.0	11±8.2
<i>A. pomorum</i>	7.8±0.4	3.5±1.8
<i>L. brevis</i> EW	No inhibition	5.4±2.4
<i>L. plantarum</i> WJL	8.0±4.3	8.9±2.3

Cecropin A1 and Diptericin resistance activities are expressed as relative CFUs on plates with the number of colony-forming units in the untreated bacteria arbitrarily set to 100%. Data represent means ± SEM ($n = 3$).

Table 6. HOCl resistance of the isolated gut and established bacteria

Bacterial strains	HOCl 15 µg/L	HOCl 50 µg/L
	– Resistance activity (%) –	
<i>A. persici</i> SK1	110 ± 12	84 ± 12
<i>A. indonesiensis</i> SK2	110 ± 10	36 ± 1.1
<i>L. pentosus</i> SK3	87 ± 9.5	9.3 ± 1.3
<i>P. rettgeri</i> SK4	130 ± 7.0	56 ± 2.9
<i>Gluconobacter morbifer</i> G707T	105 ± 3.0	87 ± 10
<i>Commensalibacter intestini</i> A911T	77 ± 3.6	0.0 ± 0.0
<i>A. pomorum</i>	124 ± 11	112 ± 0.8
<i>L. brevis</i> EW	104 ± 2.7	101 ± 0.6
<i>L. plantarum</i> WJL	97 ± 2.1	83 ± 6.0
<i>Ecc15</i> 2141	100 ± 8.5	100 ± 11
<i>P. azotoformans</i> IAM1603	100 ± 1.8	19 ± 1.4
<i>E. coli</i> K12	69 ± 11	0.3 ± 0.1
<i>P. alcalifaciens</i> JCM1673T	6.6 ± 1.1	0.0 ± 0.0

HOCl resistance activity is expressed as relative CFUs on plates with the number of colony-forming units in the untreated bacteria arbitrarily set to 100%. Data represent means ± SEM ($n = 3$).

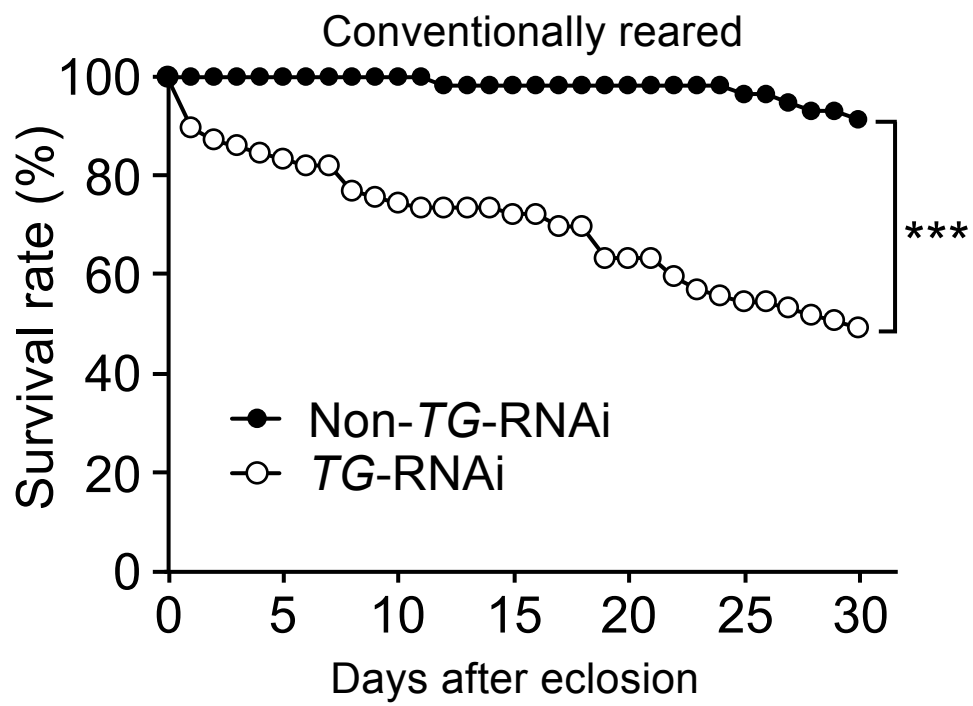


Figure 1

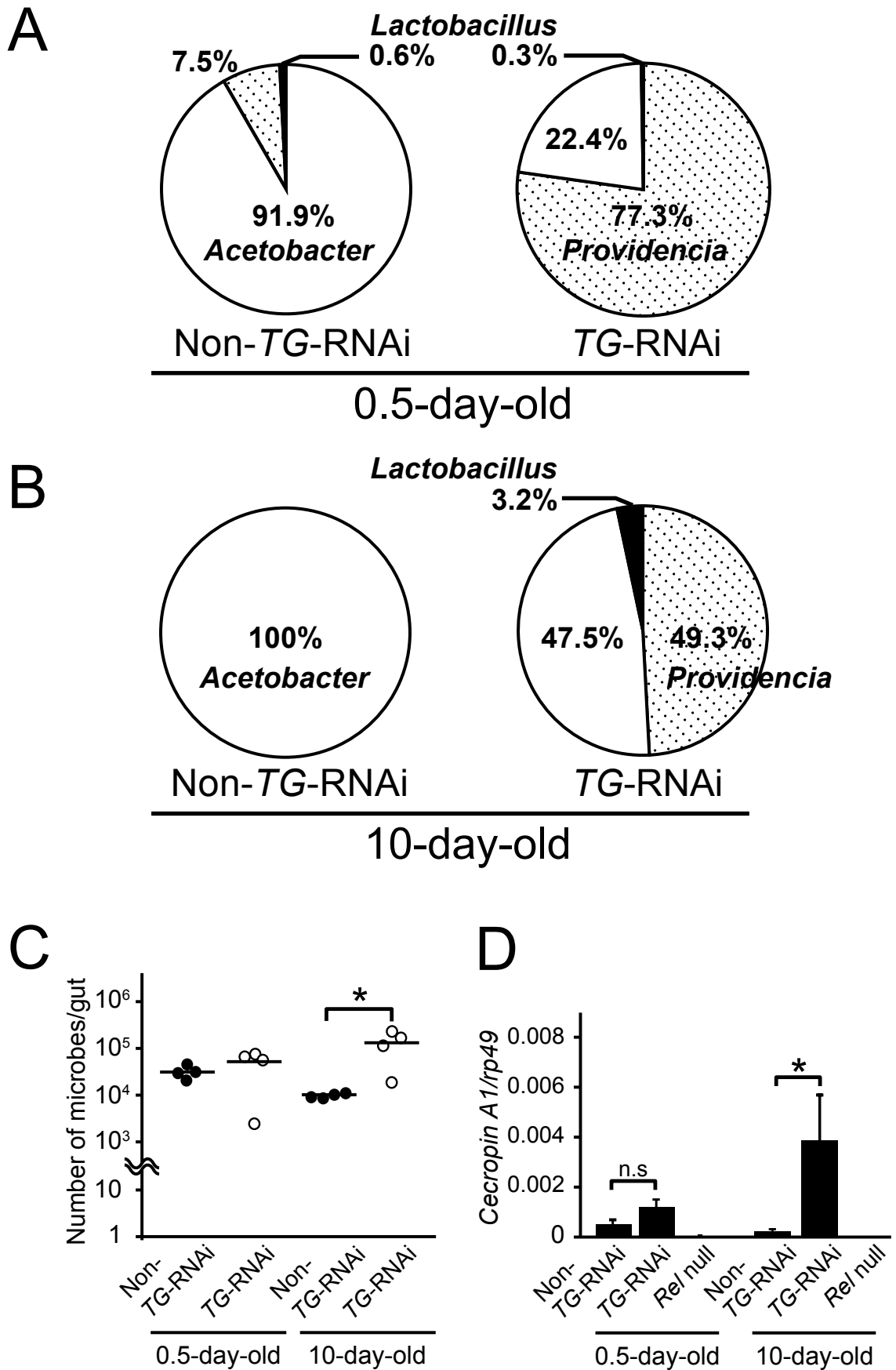


Figure 2

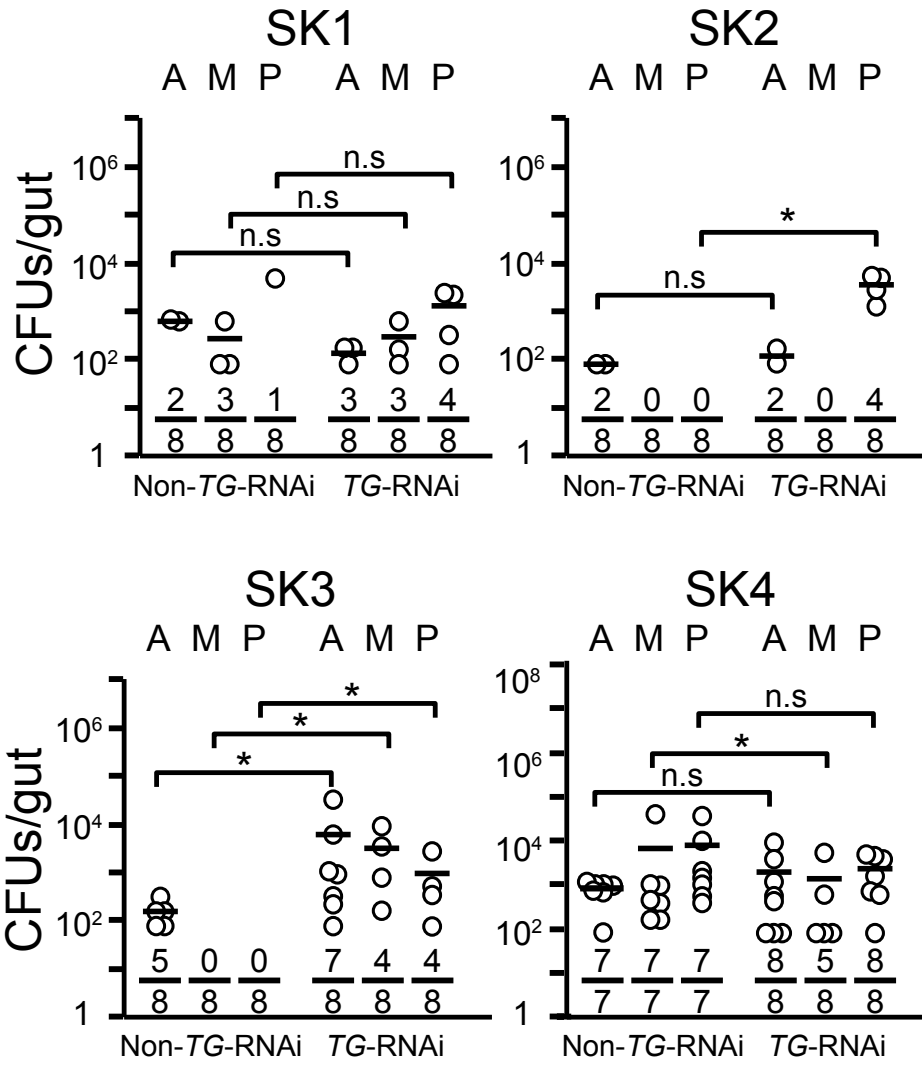
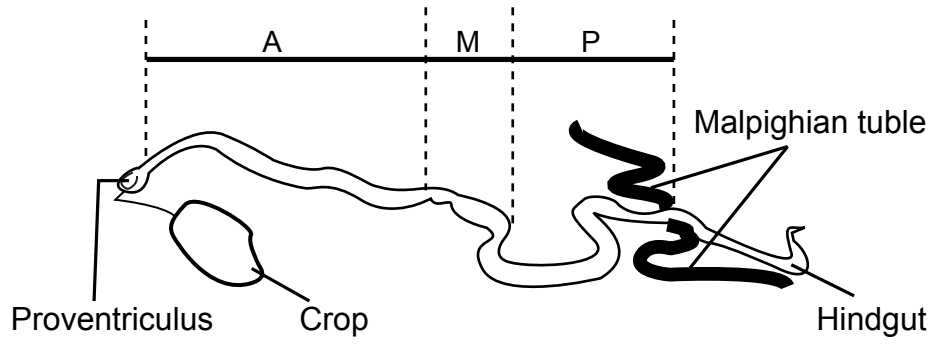


Figure 3

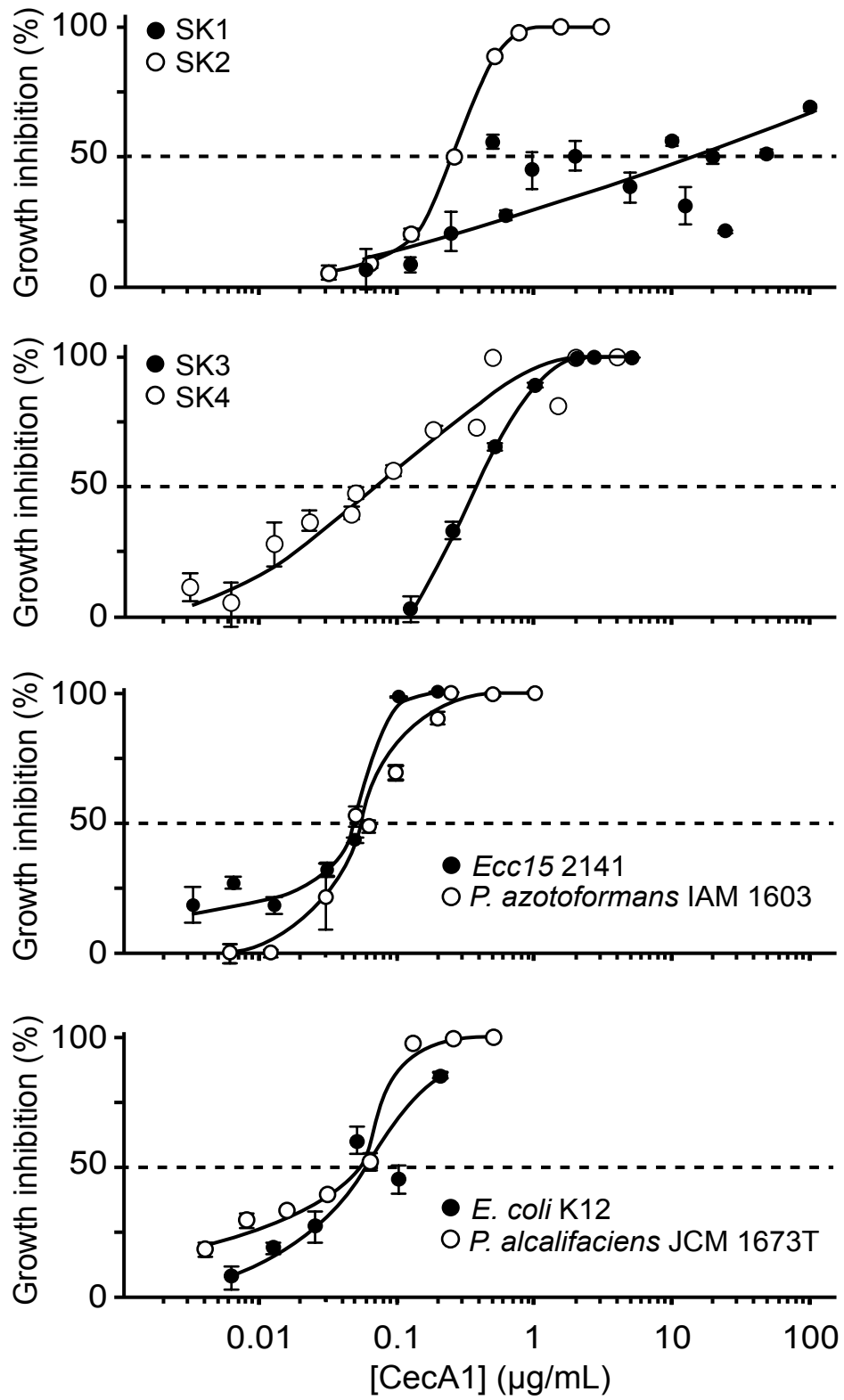


Figure 4

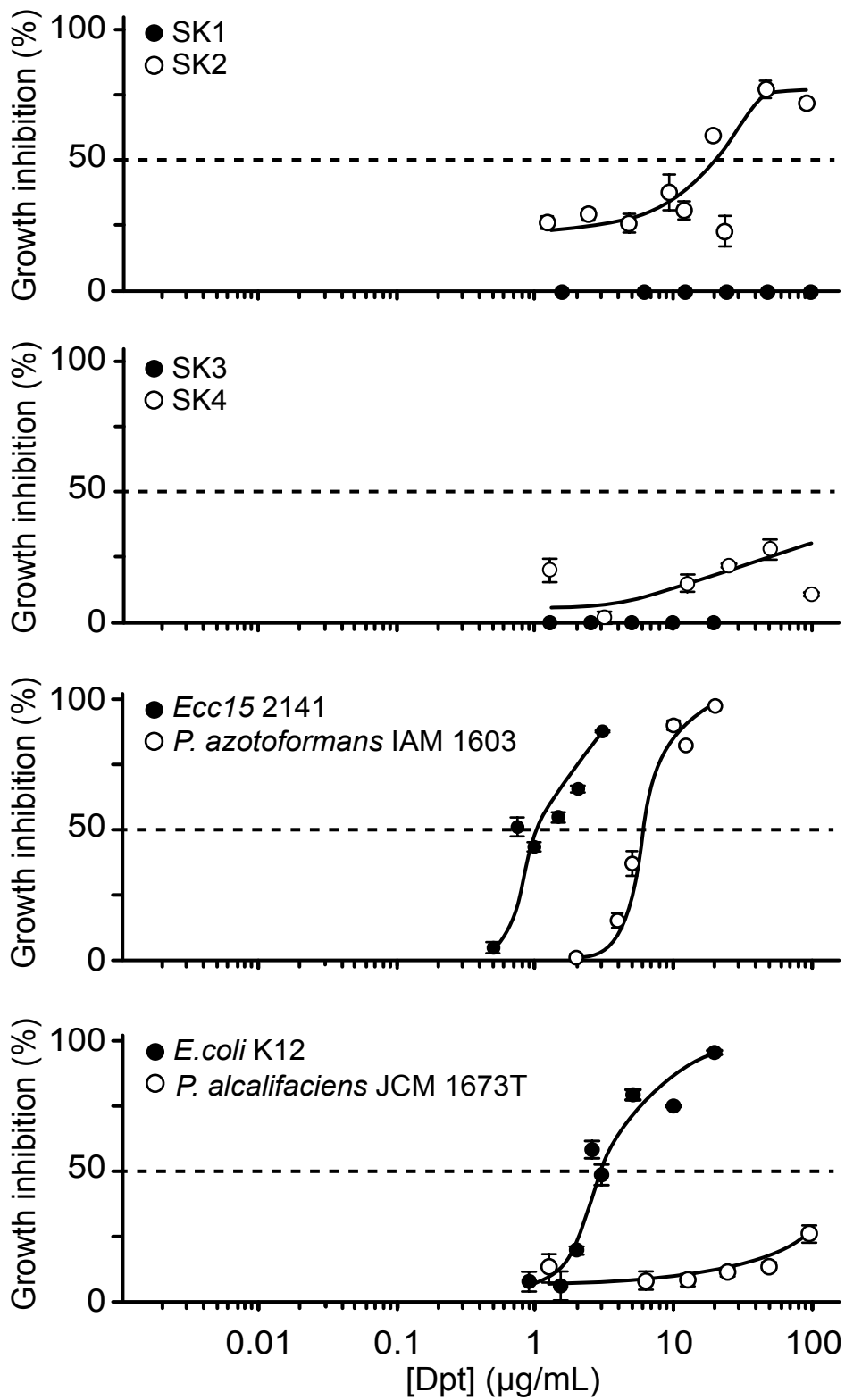


Figure 5

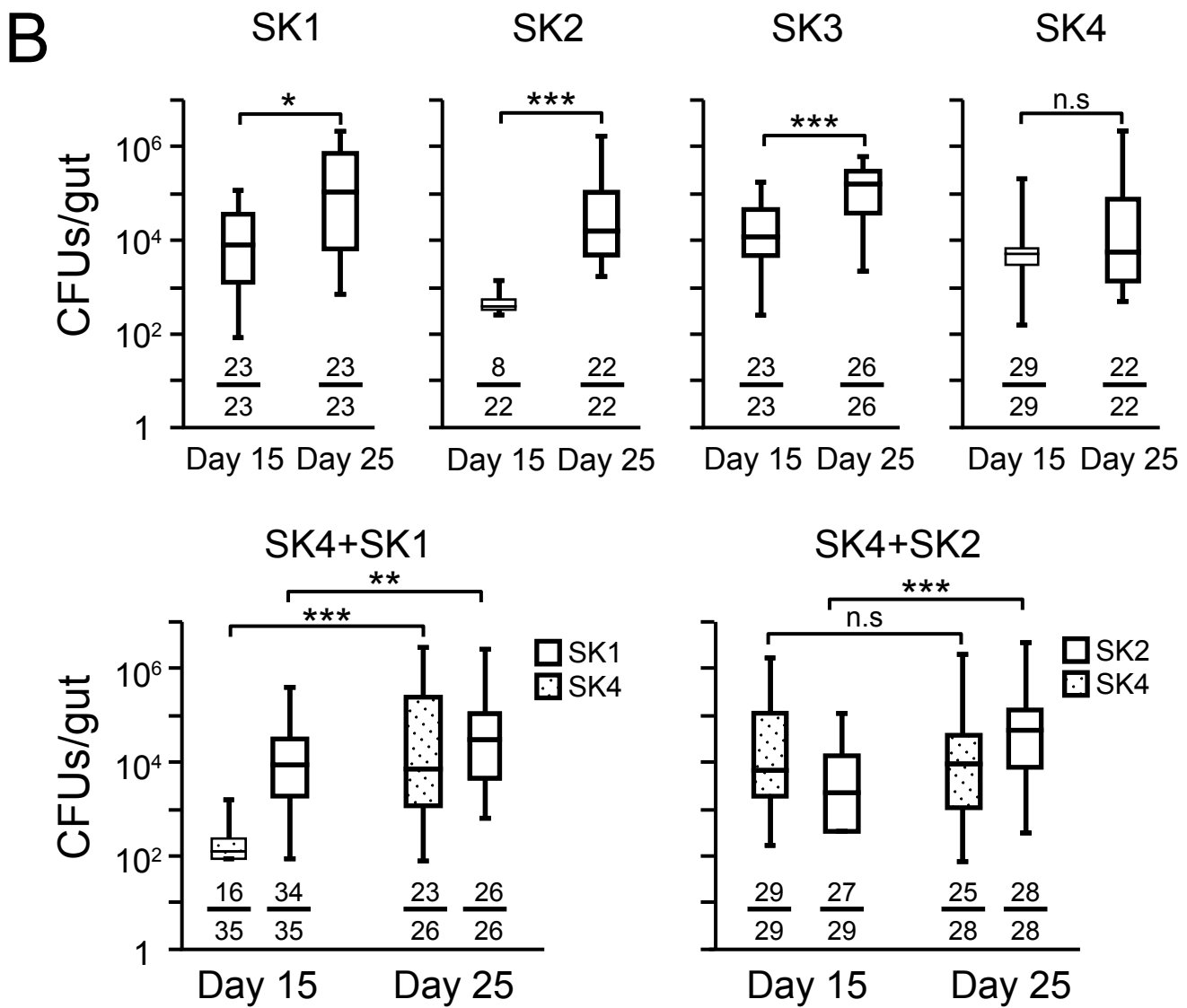
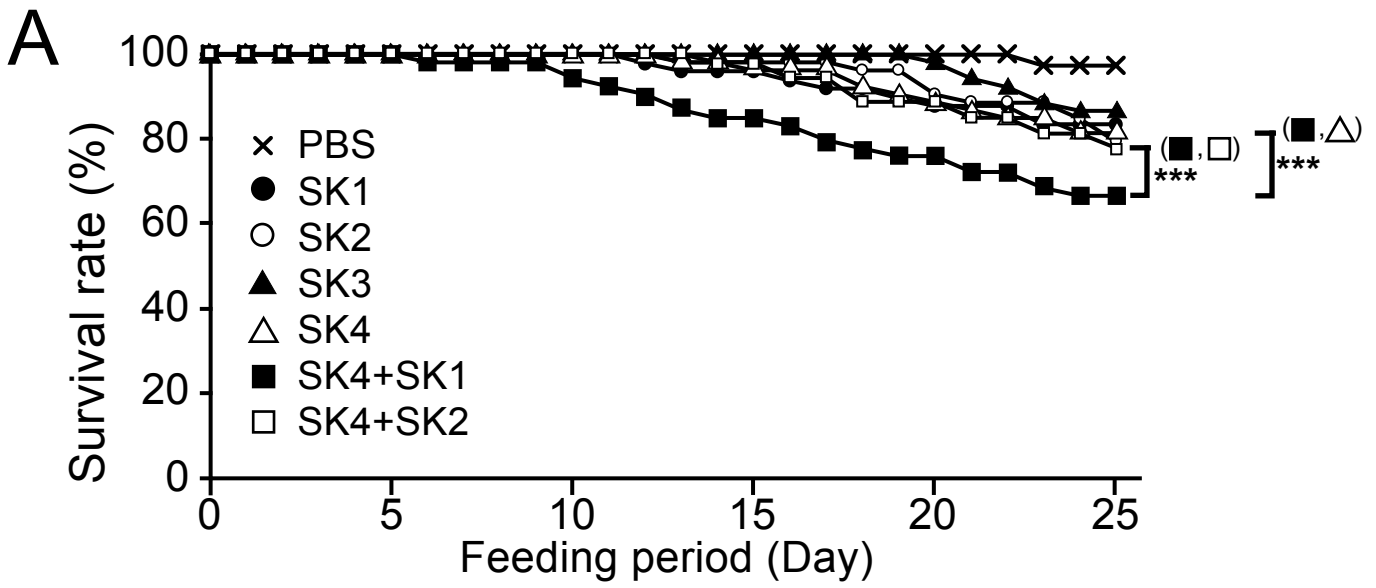


Figure 6

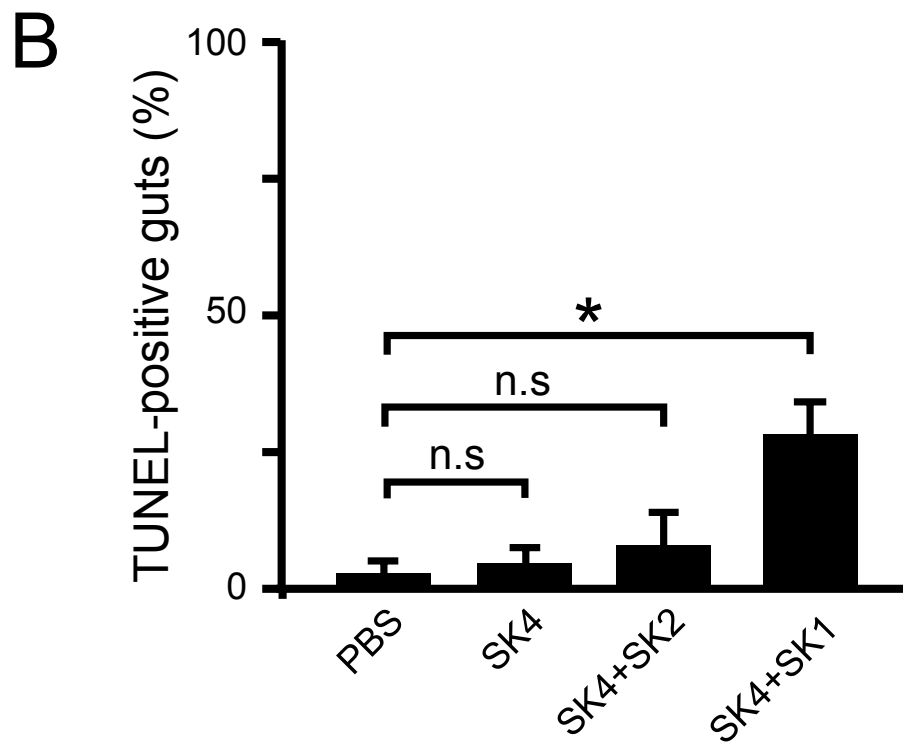
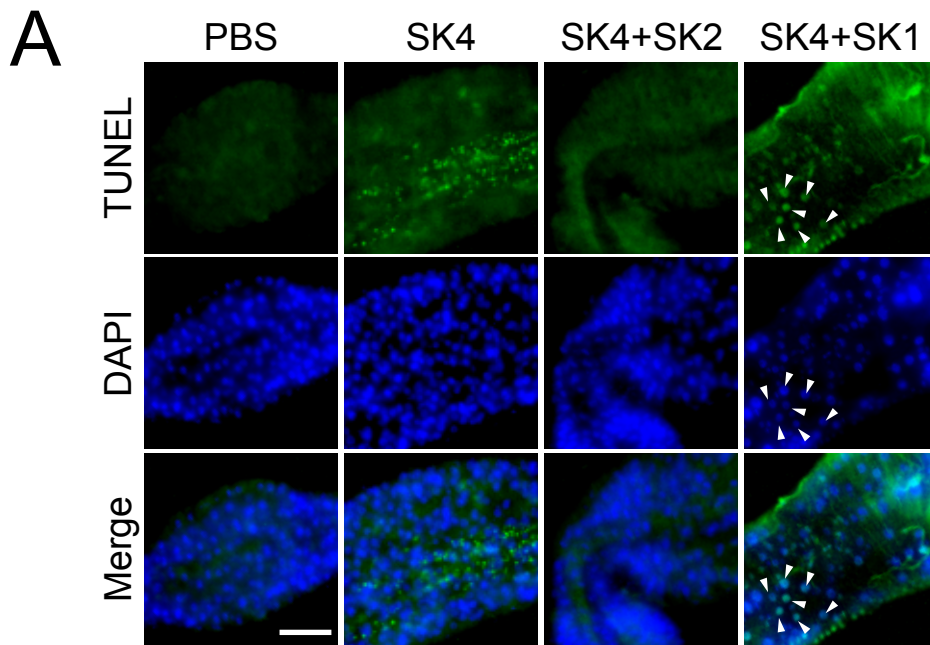


Figure 7

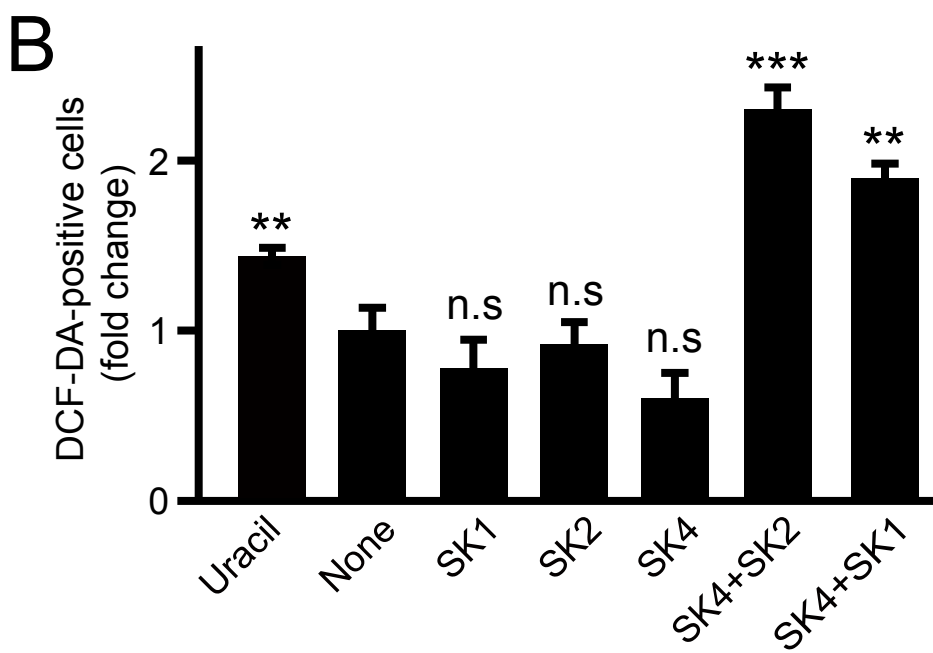
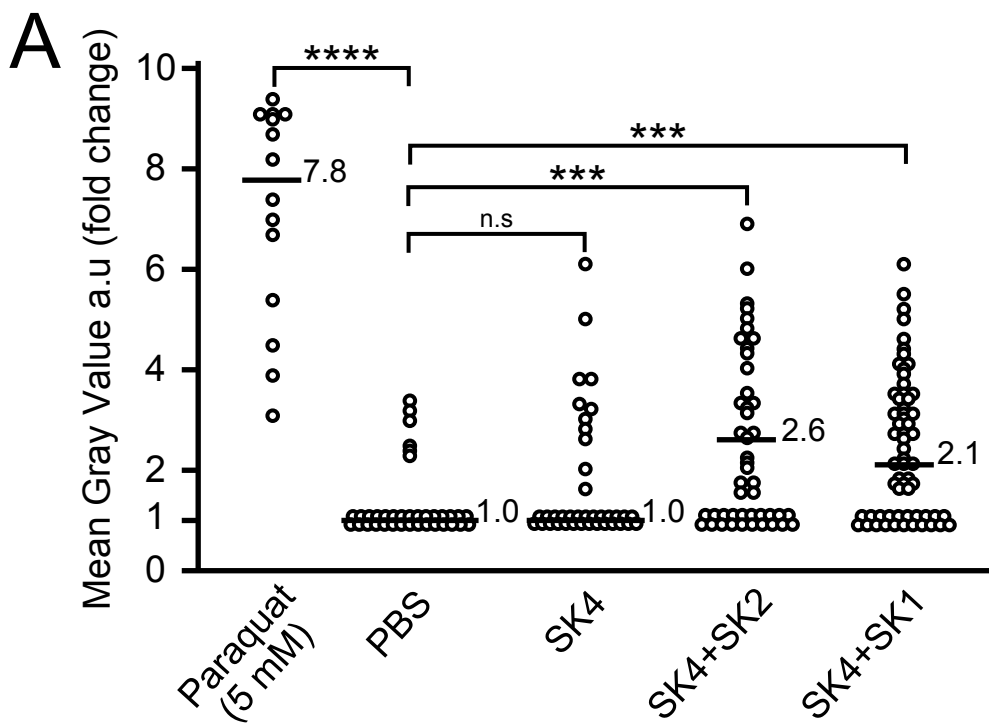


Figure 8

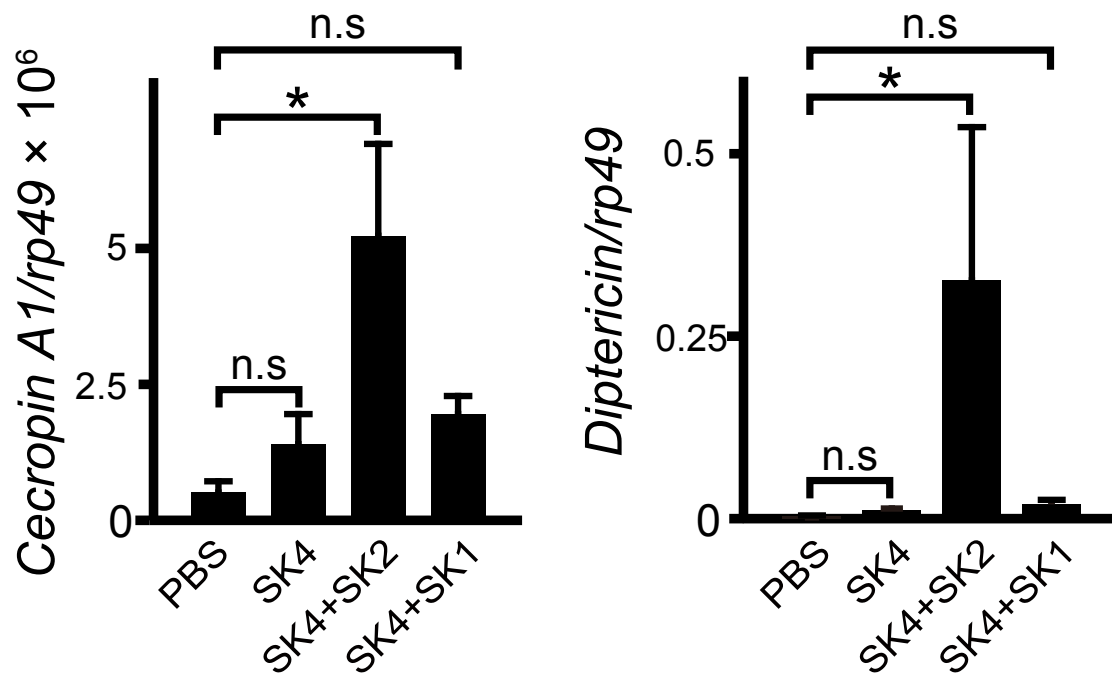


Figure 9

ACKNOWLEDGEMENTS

First and foremost, I wish to express my sincere gratitude to Professor Shun-ichiro Kawabata (Kyushu University) for all his effort, time and patience in helping me to complete this thesis. Without his continuous support and understandings, the completion of this dissertation would have not been possible. Secondly, I especially appreciate Dr. Toshio Shibata (Kyushu University) for his valuable advice and support on my dissertation. I would like to thank again for their constructive suggestions and useful critiques. I would also like to express my gratitude to all other current and past lab members.

I am grateful to Dr. Ryu Ueda (National Institute of Genetics, Mishima, Japan) for providing the fly strains. I am also grateful to Drs. Shoichiro Kurata (Tohoku University), Takayuki Kuraishi (Kanazawa University), and Won-Jae Lee (Seoul national University, Seoul, Korea) for providing the bacterial strains, and Drs. Takumi Koshihara (Kyushu University) and Takeshi Ishihara (Kyushu University) for helpful discussions regarding this study.

Special thanks goes to my sisters, friends, and individuals for their support and encouragement through the years. In particular, I must acknowledge my parents. I would like to dedicate this thesis to my mother Hiroko and my father Yuichi who supported and encouraged me through all these years of studying.